It is easily seen that

$$I = \frac{1}{2}\int d^3x \, dt\left[\psi^*i\frac{\partial}{\partial t}\psi - \psi i\frac{\partial}{\partial t}\psi^* - \psi^*H\psi - \psi H\psi^*\right], \quad (51)$$

is a variational expression for $\psi$ and $\psi^*$. We propose to use it to determine the cross sections in the intermediate region.[16] A reasonable form for $\psi$ in this region would be a sum of the high- and low-energy forms:

$$\psi = \alpha_+(t)\chi_0^+ + \alpha_-(t)\chi_0^- + \beta_+(t)\phi_0(\mathbf{x}+\tfrac{1}{2}\mathbf{R})$$
$$\times \exp[-\tfrac{1}{4}i\mathbf{x}\cdot d\mathbf{R}/dt - i\eta_0(t)] + \beta_-(t)\phi_0(\mathbf{x}-\tfrac{1}{2}\mathbf{R})$$
$$\times \exp[\tfrac{1}{4}i\mathbf{x}\cdot d\mathbf{R}/dt - i\eta_0(t)]. \quad (52)$$

[16] This technique has been used recently in the low-energy region by N. C. Sil, Proc. Roy. Soc. (London) 75, 194 (1960).

Such a form could be used in (51) with the 4 variational functions $\alpha_\pm$, $\beta_\pm$ to determine the exchange to the ground state. Such a calculation is now in progress and will be reported on subsequently.

# Ionization Produced by Atomic Collisions at kev Energies. III*

J. B. Bulman† and A. Russek
*University of Connecticut, Storrs, Connecticut*
(Received December 13, 1960)

The electron evaporation model of the collision-ionization process that occurs when atoms collide at high energies is extended to include atoms with from two to eight electrons in the outer shell. Application of the model to data from collisions of $N^+$ on Ar and $Ne^+$ on Ar gives evidence for a resonant electron capture effect taking place in high-energy violent collisions which was heretofore masked by the multiple ionization consequent on such collisions.

## 1. INTRODUCTION

TO account for ionization produced by violent atomic collisions, a phenomenological theory was developed in two previous papers,[1,2] hereafter referred to as I and II. These papers were restricted in scope to the collisions of atoms with outer shells of eight electrons (i.e., the noble gases). Since that time some experimental data have been published for collisions involving nitrogen ions (with five electrons). It was therefore decided to extend the theory to include atoms with from two to eight electrons in the outer shell. In addition, the evaporation theory will be used to show evidence of resonant electron capture, in violent ion-atom collisions.

The theory, as originally developed in I, utilizes an evaporation model of the collision-ionization process. As the two charge distributions sweep through each other, a small amount of kinetic energy of translation of the atoms is transferred to their internal degrees of freedom by a friction-like mechanism. This energy (ordinarily called the "inelastic energy") is assumed to be statistically distributed among the outer-shell electrons of the atoms. Then, upon separation, the "heated" atoms get rid of this excess energy, partly by photon emission and partly by electron evaporation.

In the previous work, ionization probabilities were calculated only for atoms having eight outer electrons and the resulting ionization probability curves compared very closely with the experimental curves for $Ar^+$ on Ar scattering. In Sec. 2 of the present work, ionization probability curves are calculated for atoms having from two to seven electrons in the outer shell. When the five-electron curves are compared with $N^+$ on Ar scattering data, the agreement is good, indicating that the evaporation model need not be restricted to the noble-gas atoms, but has validity in other cases as well.

Recent experiments[3,4] have shown evidence for a resonant capture process occurring in ion-neutral atom collisions. Clear-cut evidence for the resonant capture effect was found in collisions involving the very light atoms and for the heavier atoms only in the very gentle collisions. Resonant capture effects, if they occur in the more violent collisions of the heavier atoms, are masked

[1] A. Russek and M. T. Thomas, Phys. Rev. 109, 2015 (1958).
[2] A. Russek and M. T. Thomas, Phys. Rev. 114, 1538 (1959).
[3] F. P. Ziemba and E. Everhart, Phys. Rev. Letters 2, 229 (1959).
[4] F. P. Ziemba, G. J. Lockwood, G. H. Morgan, and E. Everhart, Phys. Rev. 118, 1552 (1960).
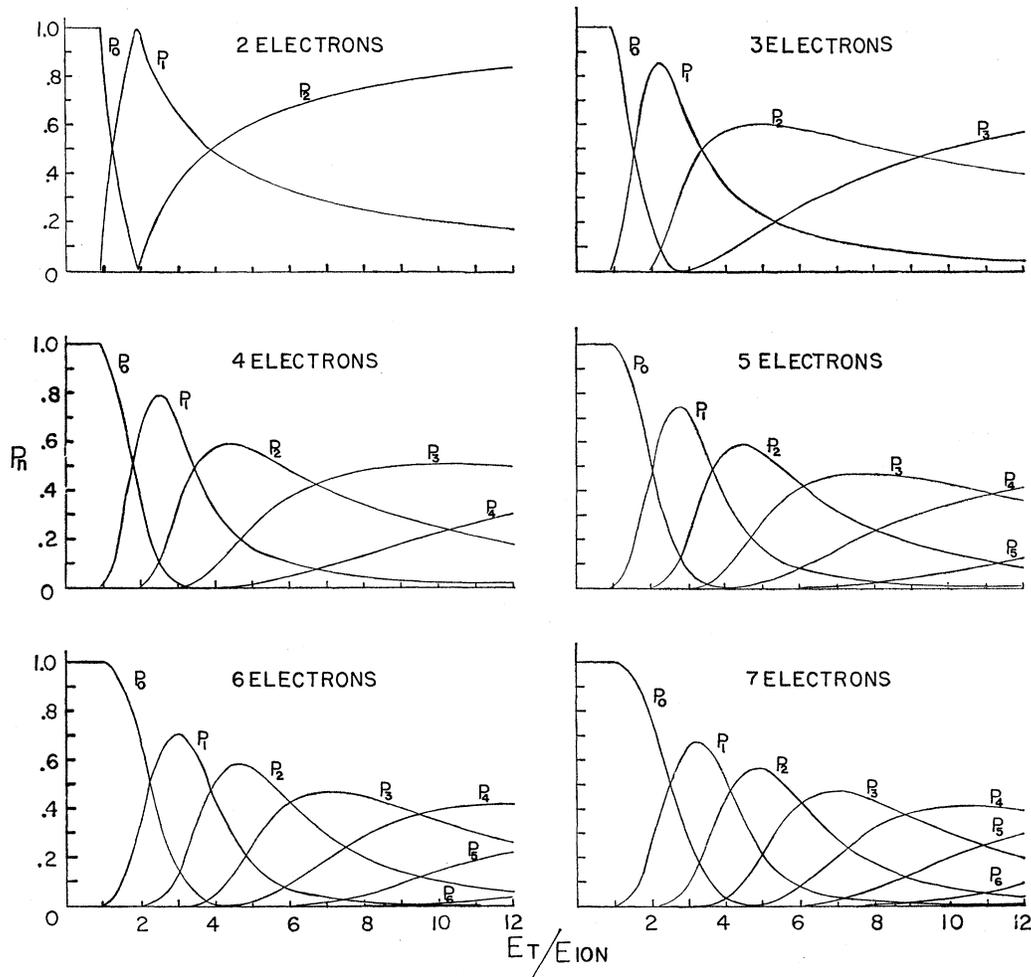
FIG. 1. The ionization probabilities for neutral atoms containing from two to seven electrons in the outer shell are plotted as functions of the energy $E_T$ transferred to the internal degrees of freedom. The energy is given in units of size $E_{ion}$, the average ionization potential for electrons in the outer shell.

by the multiple ionization which is also taking place. With the help of the evaporation model, however, resonant capture effects clearly show up through the multiple ionization effect. Specifically, in Sec. 3 of the present paper, the probability that the incoming ion picks up an electron from the neutral target atom is *not* assumed to be 0.5 as in reference 1, but is determined empirically as a function of the collision parameters by best fit of the evaporation theory with the experimental data. The probability for electron capture as determined in this way clearly shows evidence for resonant electron capture effects.

## 2. EXTENSION OF THE EVAPORATION MODEL

The distribution-in-energy among the outer electrons was effected in I by dividing the energy scale into cells of equal width $\epsilon$ and then calculating the ionization probability curve algebraically. The size of the energy cell was there taken to be one-quarter of the ionization

energy. The statistics were improved in II by going to the limit $\epsilon \to 0$. The resulting curves were almost coincident with the original curves except for a lateral shift to slightly higher values of $E_T$. Thomas[5] shows that the limiting curves are quickly approached as the cell size is decreased. The curves presented here are calculated algebraically using an energy cell size equal to one-tenth the ionization energy which, for all practical purposes, is the limiting case. A uniform ionization potential for all outer electrons is again assumed. Ionization probability curves are calculated for the cases of two electrons up to seven electrons in the outer shell. The appropriate generalization of Eq. (2) in I is

$$P_n{}^N(m)$$

$$= \binom{N}{n} \sum_{i=0}^{m-10n} K_n(i) Q_{N-n}{}^{10}(m-10n-i)/K_N(m). \quad (1)$$

[5] M. T. Thomas, M.S. thesis, University of Connecticut, Storrs, Connecticut (unpublished).

Here, $P_n{}^N(m)$ is the probability that a neutral atom having $N$ outer electrons will become $n$-fold ionized when the energy transferred to the $N$ electrons during the collision is $m\epsilon$. Also, $\binom{N}{n}$ is the binomial coefficient, $K_n(m)$ is the total number of ways in which the energy $m\epsilon$ can be distributed among the $n$ electrons, and $Q_n{}^{10}(m)$ is the number of ways the energy $m\epsilon$ can be divided among $n$ electrons such that none have $10\epsilon$ or more energy. The quantities $K_n$ and $Q_n{}^{10}$ are calculated using the same recursion relationships given in I.

The resulting probability curves thus calculated are shown in Fig. 1 as functions of the energy transferred. The values of the corresponding peak heights and intersection heights for the different sets of curves are approximately the same as for the eight-electron curves, as can be seen in Table I. Thus the theory predicts that there will be no marked difference in the character of the ionization curves plotted as functions of the inelastic energy of the collision as applied to successive atoms in the periodic table. The probability curves just calculated have assumed that the incident atom is neutral. Most of the presently available data, on the other hand, are for an incident projectile atom already singly ionized. Letting $a$ denote the probability that an electron will be transferred from the target to the incident ion during the collision, then the probability $\tilde{P}_n$ that the incident ion is $n$ times ionized after a scattering becomes

$$\tilde{P}_n = aP_n{}^N + (1-a)P_{n-1}{}^{N-1}. \tag{2}$$

The two terms on the right side of Eq. (2) account for the two possibilities for the scattered particle to become $n$ times ionized. First the incident ion could capture an electron and then evaporate $n$ electrons from the $N$ electrons in the outer shell, or secondly, if no electron capture takes place, the incident ion could

TABLE I. Heights of intersections and peaks of the theoretical ionization probability curves for neutral atoms with $N$ outer electrons.

| Intersection or peak | $N=8$[a] | $N=7$ | $N=6$ | $N=5$ | $N=4$ | $N=3$ | $N=2$ |
|---|---|---|---|---|---|---|---|
| $P_1 \times P_0$ | 0.50 | 0.50 | 0.50 | 0.50 | 0.50 | 0.49 | 0.48 |
| $P_1$ | 0.63 | 0.67 | 0.70 | 0.74 | 0.79 | 0.86 | 1.00 |
| $P_2 \times P_0$ | 0.18 | 0.16 | 0.15 | 0.13 | 0.10 | 0.07 | 0.00 |
| $P_3 \times P_0$ | 0.03 | 0.03 | 0.02 | 0.01 | 0.01 | 0.00 | ... |
| $P_2 \times P_1$ | 0.47 | 0.46 | 0.48 | 0.48 | 0.49 | 0.49 | 0.50 |
| $P_2$ | 0.55 | 0.57 | 0.58 | 0.59 | 0.59 | 0.60 | ... |
| $P_3 \times P_1$ | 0.23 | 0.21 | 0.21 | 0.20 | 0.20 | 0.20 | ... |
| $P_4 \times P_1$ | 0.07 | 0.08 | 0.08 | 0.08 | 0.07 | ... | |
| $P_3 \times P_2$ | 0.42 | 0.42 | 0.42 | 0.42 | 0.42 | 0.47 | |
| $P_5 \times P_1$ | 0.02 | 0.03 | 0.03 | 0.03 | ... | ... | |
| $P_3$ | 0.47 | 0.47 | 0.47 | 0.47 | 0.51 | ... | |
| $P_4 \times P_2$ | 0.24 | 0.24 | 0.24 | 0.24 | 0.24 | ... | |
| $P_6 \times P_1$ | 0.01 | 0.01 | 0.01 | ... | ... | ... | |
| $P_4 \times P_3$ | 0.38 | 0.37 | 0.37 | 0.39 | ... | ... | |
| $P_5 \times P_2$ | 0.12 | 0.12 | 0.12 | 0.11 | ... | ... | |
| $P_4$ | 0.41 | 0.40 | 0.42 | ... | ... | ... | |
| $P_6 \times P_2$ | 0.06 | 0.05 | 0.05 | ... | ... | ... | |
| $P_5 \times P_3$ | 0.25 | 0.25 | 0.25 | ... | ... | ... | |

[a] Calculated by Thomas (see reference 5) with cell size $\epsilon \to 0$.
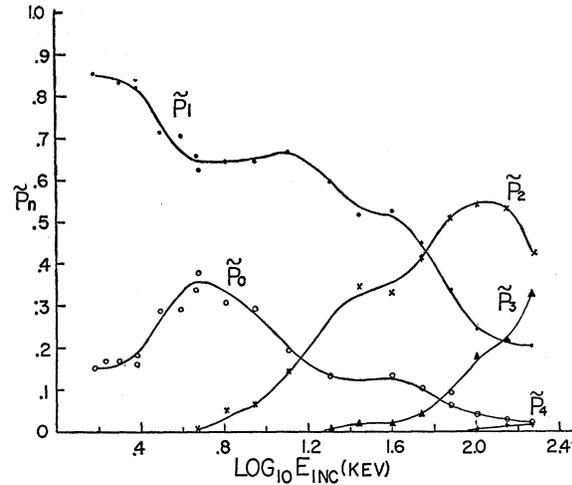


FIG. 2. The charge analysis vs incident ion energy for collisions of nitrogen ions on argon atoms. The fractions $\tilde{P}_n$ of the scattered ion beam in the various states of ionization are plotted against the logarithms of the incident ion energy in kev. The scattered beam is measured at the fixed angle of scattering of 5 degrees.

evaporate $n$-1 electrons from the $N$-1 electrons in the outer shell. Thus, $a$, as a function of the collision parameters, is the charge transfer probability.

For a violent atomic collision, where the distance of closest approach of the two nuclei is small, a value of $a$ equal to one-half may reasonably be expected for collisions between identical species. Actually it will be shown later that experimental data strongly suggest that the charge transfer cross section varies somewhat with the collision parameters. The five electron curves calculated using Eq. (2) and a constant charge transfer probability of one-half can be compared directly with the experimental N$^+$ on Ar scattering data[6] at a constant scattering angle of 5°. These data, shown in Fig. 2, give the charge analysis of an initially singly ionized nitrogen beam after scattering through five degrees from a gas of neutral argon. The incident ion energies range from 1 kev to 183 kev. The percentage of the scattered beam in the various states of ionization is plotted here against the logarithm of the incident energy in order to compress the energy scale. As a check on agreement with experiment, a comparison of the peak heights and intersection heights of the data and the five-electron ionization probability curves using $a$ equal to one-half in Eq. (2) (as assumed in I) is given in Table II. Except for two points, the agreement is fairly good, indicating that the electron evaporation model can account for ionization produced in violent atomic collisions for other atoms as well as the noble gases originally considered. Very much the same general type of ionization curves may be expected for atoms independent of the number of outer shell electrons.

It should be noted that in the work using Ar$^+$ on

TABLE II. Peak heights and intersection heights of calculated and experimental probability curves, for $N^+$ on Ar, 5-deg scattering.

|  | Experimental | Calculated |
|---|---|---|
| $P_2 \times P_0$ | 0.17 | 0.29 |
| $P_2 \times P_1$ | 0.43 | 0.41 |
| $P_3 \times P_0$ | 0.06 | 0.08 |
| $P_2$ | 0.54 | 0.45 |
| $P_4 \times P_0$ | 0.02 | 0.01 |
| $P_3 \times P_1$ | 0.22 | 0.26 |
| $P_3 \times P_2$ | 0.37 | 0.39 |

Ar, the data gave the ionization probabilities for a constant incident ion energy at various scattering angles. The present $N^+$ on Ar data give the ionization probabilities at various incident ion energies for a constant scattering angle. Since only peak heights and intersection heights are being compared, no energy-transferred relationship is needed. However, in the next section, when a comparison between experiment and theory is made over the entire curves, a relation between energy transferred and incident ion energy will have to be assumed. This will be an empirical relation inasmuch as the functional dependence of the inelastic energy on the collision parameters has not as yet been measured directly, and the theoretical estimates made in I are not good enough for the present purposes.

### 3. EVIDENCE FOR RESONANT ELECTRON CAPTURE

Differential scattering measurements by Ziemba and Everhart[3] and by Ziemba et al.[4] for $He^+$ on He at five degrees scattering angle revealed several resonant peaks when the fraction of incident ions which captured an electron to become neutral was plotted as a function of the incident ion energy in the range of from 2 kev to 250 kev. A similar phenomenon was also found in other combinations of light ion-atom collisions.

This same type of resonant electron capture may take place when heavier ions collide in violent collisions, but the phenomenon is masked by multiple ionization
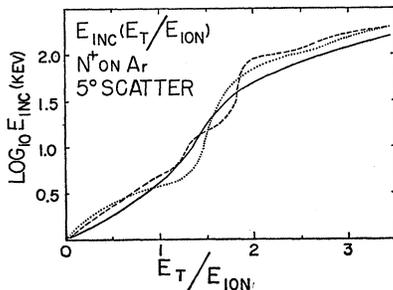


FIG. 3. The energy transferred to the internal degrees of freedom $E_T$ is shown as a function of the incident ion energy. The solid curve gives the best agreement with $N^+$ on Ar data when used together with the solid curve of Fig. 4, in Eq. (3). The dotted curve gives best agreement with experiment when $a$ is taken to be constant at 0.25 in Eq. (3). The broken curve gives best agreement with experimental data when used together with the broken curve of Fig. 4, in Eq. (3).
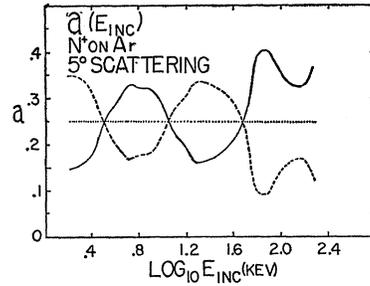


FIG. 4. The charge transfer probability vs the incident ion energy for $N^+$ on Ar at 5-degree scattering. The solid curve, when substituted into Eq. (3), gives the best agreement with experimental results. The constant value of $a$ equals 0.25 and the broken curve gives progressively poorer agreement.

which is also taking place. Evidence for this resonant charge transfer in these high-energy regions will now be presented.

To compare the $N^+$ on Ar scattering data shown in Fig. 2, giving the ionization probabilities as functions of the incident ion energy, with the calculated evaporation curves which give the ionization probabilities as functions of $E_T/E_{ion}$, a relationship is obtained empirically between the incident ion energy, $E_{inc}$, and the energy transferred during collision, $E_T/E_{ion}$. This relation is shown as the solid line in Fig. 3.

When $a$ is allowed to vary with energy and the dependence is empirically adjusted to give the closest agreement between theory and the $N^+$ on Ar scattering data, better agreement is obtained than is possible with a constant value of $a$. The error averaged over all curves is found to be only 0.022. This is much lower than is possible with any constant value of $a$. The function of charge transfer probability versus incident ion energy giving this agreement is shown as the solid curve in Fig. 4. This function, when used in the expression

$$\tilde{P}_n = aP_n{}^5 + (1-a)P_{n-1}{}^4 \tag{3}$$

(where it must be remembered that $a$ is a function of the incident ion energy), gives the curves shown in Fig. 5. Experimental points are also shown and the agreement can be seen to be quite good.

The sensitivity of the ionization probability curves to the charge transfer probability $a$ and to the energy transferred $E_T$ is now shown. What we do, in effect, is to select a one-parameter family of charge transfer probability curves, one of which is the "best fit" curve. For each of the charge transfer probability curves shown in Fig. 4 the best energy-transferred function is obtained that optimizes agreement with the data for that particular charge transfer probability function. These three optimal curves for $E_T$ are shown in Fig. 3, the solid curve of Fig. 3 corresponding to the solid curve of Fig. 4, and so forth. Figure 5 shows the agreement of the evaporation theory with experiment when the best fit (solid) curves are used.
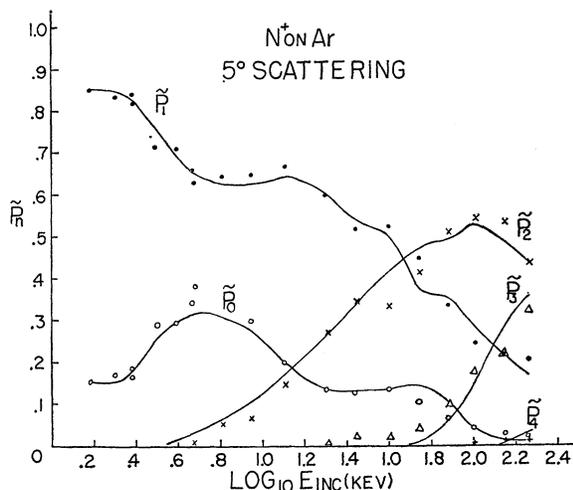
It is seen from Figs. 3 and 4 that widely differing

FIG. 5. Ionization probability curves for $N^+$ on Ar calculated with Eq. (3) using the charge transfer probability given by the solid curve in Fig. 4 and the energy-transferred function given by the solid curve in Fig. 3. The experimental points are also shown for comparison.

charge transfer probabilities do not result in substantially different energy-transferred functions. The latter are essentially determined by the multiple ionization effects. Table III below gives the average errors when the ionization probabilities for each of the three charge transfer probabilities, each with its optimum energy-transferred function, are compared with the experimental data. This average error is computed by taking the mean of the absolute values of the differences between each experimental point in Fig. 5 and the value of the theoretical curve at that incident ion energy.

## 4. DISCUSSION OF RESULTS

A casual glance might leave the reader with the impression that if enough empirically determined functions are used, a theory can be made to fit any data. It is, therefore, worthwhile to discuss the results obtained above with a view to showing just how much of the agreement is due to empirical fit and how much is intrinsically contained in the theory. The evaporation theory of multiple ionization produced by ion-atom collisions requires two functions of the collision parameters: the energy transferred, $E_T$, and the capture probability, $a$. Each of these should eventually be predicted by a priori reasoning, but, for the time being, they have been empirically determined.

It should be borne in mind, however, that the principal features of the multiple ionization curves can be adequately accounted for with any reasonable capture probability $a$. Good agreement was obtained in I (for $Ar^+$ on Ar) and in Sec. 2 of the present work (for $N^+$ on Ar) with a constant capture probability of one-half, even though one would not even expect the constant to be one-half in the case of collisions between dissimilar species. In Sec. 3 of the present work (see

TABLE III. Comparison of theory with experiment for $N^+$ on Ar, 5° scattering data, when $a$ is empirically determined to give best over-all fit and when it differs from the best fit values.

| $a(E_{inc})$ | $E_{inc}(E_T)$ | Average error |
| --- | --- | --- |
| solid curve, Fig. 4 | solid curve, Fig. 3 | 0.022 |
| dotted curve, Fig. 4 | dotted curve, Fig. 3 | 0.048 |
| dashed curve, Fig. 4 | dashed curve, Fig. 3 | 0.076 |

Table III), with a constant value $a=0.25$, the average discrepancy between theoretical curves and the experimental points is 0.048, while the curves themselves range between 0 and 0.5.

With this measure of success established it is only reasonable, as a next step, to let $a$ itself vary and to find its dependence on the collision parameters empirically. This too was done in Sec. 3. The empirical fit for best agreement unambiguously determined the general features of the functional dependence of $a$ on the incident ion energy to be the one shown in the solid curve of Fig. 4. (The exact values should not be taken too seriously, just the over-all shape.) This function for $a$ dropped the average disagreement between theory and experiment from 0.048 to 0.022. Effectively what is being done in this empirical adjustment is to bring the theoretical $P_0$ curve into agreement with the experimental values. The remaining ionization probability curves are then automatically predicted by the evaporation theory and give the agreement just mentioned. Significantly enough, the functional dependence of $a$ on the incident ion energy has two peaks, indicative of a resonance capture phenomenon similar to that found by Ziemba et al. for many combinations of lighter atoms. Moreover, when the spacing between peaks is converted into time of collision, as was done in reference 4, these times fit into the same pattern
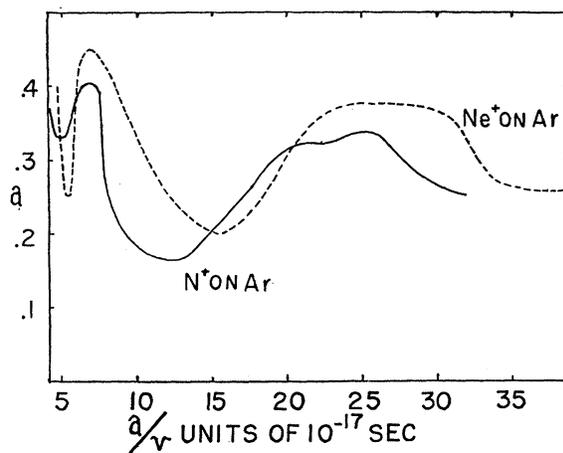


FIG. 6. The empirically determined charge transfer probability values which give best agreement with the experimental data for $N^+$ on Ar and $Ne^+$ on Ar are shown plotted as functions of the collision time. The $N^+$ on Ar curve is shown as the solid curve while the $Ne^+$ on Ar curve is shown as the broken curve. The general behavior of both curves is quite similar.
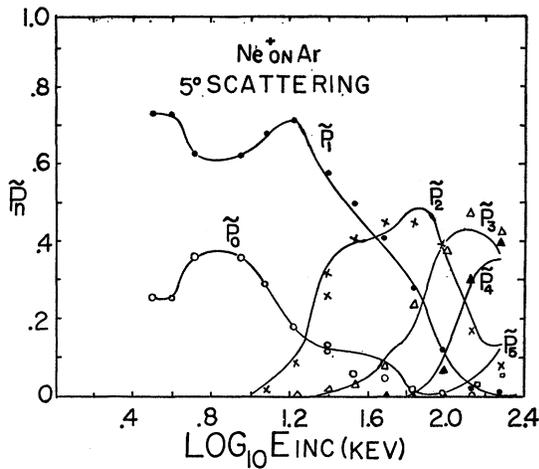
FIG. 7. Ionization probability curves for Ne+ on Ar calculated with Eq. (3) using the charge transfer probability shown in Fig. 6 and an empirically determined energy-transferred function. The experimental points are also shown for comparison.

established by the other combinations. These times are of the order of atomic and molecular orbital periods.

## 5. NEON-ARGON COLLISIONS

An analysis similar to that made in Sec. 3 has been performed on the data obtained in reference 4 for col-lisions of Ne+ on Ar. The charge transfer probability which optimizes agreement of the evaporation theory with the data is shown in Fig. 6 as the dashed curve. For comparison, the corresponding charge transfer proba-bility obtained in Sec. 3 for N+ on Ar is shown as the solid curve. The abscissa in Fig. 6 is $a_0/v = a_0/(2E_{inc}/M)^{\frac{1}{2}}$, which is essentially the collision time. This figure clearly shows up similarities between the two cases. The aver-age charge exchange probability for Ne+-Ar collisions is somewhat higher than for $N^+$-Ar collisions, which probably reflects the fact that Ne+ has a much greater affinity for electrons than does N+ (the respective ioni-zation potentials are 21.47 ev as compared to 14.48 ev). However, the mean capture in both cases is less than the value of 0.5 which works quite well for the collisions of Ar+ on Ar. This appears to indicate that electron capture is less likely when resonance conditions are not satisfied, although there still appear vestiges of a reso-nance-like capture.

The agreement of the theoretical curves with the experimental points obtained using the capture proba-bility curve of Fig. 6 with the best-fit energy-transferred function is shown in Fig. 7.

## ACKNOWLEDGMENTS